crystals

MDPI

*Article*

# Demonstration of C-Plane InGaN-Based Blue Laser Diodes Grown on a Strain-Relaxed Template

**Hsun-Ming Chang [1,*], Philip Chan [1], Norleakvisoth Lim [2], Vincent Rienzi [3], Michael J. Gordon [2], Steven P. DenBaars [1,3] and Shuji Nakamura [1,3]**

[1] Department of Electrical and Computer Engineering, University of California, Santa Barbara, CA 93106, USA
[2] Department of Chemical Engineering, University of California, Santa Barbara, CA 93106, USA
[3] Materials Department, University of California, Santa Barbara, CA 93106, USA
* Correspondence: hsun-ming@ucsb.edu

**Abstract:** Electrically driven c-plane InGaN-based blue edge emitting laser diodes on a strain-relaxed template (SRT) are successfully demonstrated. The relaxation degree of the InGaN buffer was 26.6%, and the root mean square (RMS) roughness of the surface morphology was 0.65 nm. The laser diodes (LDs) on the SRT laser at 459 nm had a threshold current density of 52 kA/cm$^2$ under the room temperature pulsed operation. The internal loss of the LDs on the SRT was 30–35 cm$^{-1}$. Regardless of the high threshold current density, this is the first demonstrated laser diode using the strain-relaxed method on c-plane GaN.

**Keywords:** III (Al; Ga; In)-nitrides; laser diodes; strain relaxed template; optical loss



**Citation:** Chang, H.-M.; Chan, P.; Lim, N.; Rienzi, V.; Gordon, M.J.; DenBaars, S.P.; Nakamura, S. Demonstration of C-Plane InGaN-Based Blue Laser Diodes Grown on a Strain-Relaxed Template. *Crystals* **2022**, *12*, 1208. https://doi.org/10.3390/cryst12091208

Academic Editor: Evgeniy N. Mokhov

Received: 15 August 2022
Accepted: 23 August 2022
Published: 27 August 2022



## 1. Introduction

Visible laser didoes (LDs) have sparked plenty of research interest due to their promising application in next-generation displays such as portable pico-projectors and augmented reality [1]. GaN-InN material alloys are of great interest because their bandgap spans from violet to near infrared, which is perfect for a red-green-blue (RGB) full color display module. Since the very first blue LD was demonstrated using InGaN multi-quantum wells (MQWs) as an active region by Nakamura, S. et al. [2], progress has been made to improve InGaN-based LDs and extend the wavelength longer. To date, InGaN-based blue LDs, as well as some greens, have been well developed by multiple institutions including Osram [3,4], Soraa [5,6], Nichia [7,8], ROHM [9,10], Sumitomo [11,12], UCSB [13–16], Chinese Academy of Sciences [17,18], etc.

Despite the success of blue LDs and some of the green ones, green or longer wavelength InGaN-based LDs remain challenging due to the following reasons. First, a lower growth temperature is necessary for a higher indium content InGaN because indium is considerably more volatile than GaN; however, low-temperature growth also leads to a decrease in crystalline quality [19,20]. Second, the 10% lattice mismatch between InN and GaN makes the growth of the high-Indium-content crystal difficult. The resulting high strain in InGaN can lead to misfit dislocations, phase separation and the reduction of Indium incorporation, which is also known as the composition pulling effect [21,22]. Third, due to the strong piezoelectricity in III (Al, Ga, In)-Nitrides in the c-direction, the electron and hole wavefunctions in the InGaN active region are separated, which is also known as the quantum-confined Stark effect (QCSE). This spatial separation of wavefunction overlap in turn degrades the radiative recombination efficiency and optical gain [23–25]. The requirement of an increasing indium content will exacerbate this issue due to the larger lattice mismatch and, therefore, the more severe QCSE. Furthermore, the design of the waveguide would become challenging because of the refractive index contrast reduction as the wavelength increases [26]. Although AlGaN is usually applied as bottom cladding, it suffers from the critical thickness limit and the substrate mode issue [26]. On the other

hand, InGaN, as the waveguide layer, can provide enough confinement without degrading the laser beam quality from the substrate mode. However, the demands of the high-quality growth of high-Indium-content InGaN again put emphasis on solving the InGaN growth issues, as mentioned above.

To deal with the growth issues of highly strained InGaN, growth on a strain-relaxed template (SRT) has been proposed and developed. Growth on an SRT can mitigate the lattice mismatch of the above InGaN layers (waveguide, active region, etc.) and hence the reduction of the composition pulling effect; consequently, a higher growth temperature can be used to achieve a better-quality InGaN film. Although several strain relaxation methods have been reported so far [27–30], only a few demonstrate LED device performance grown on top of them [31,32]. Recently, Chan et al. demonstrated a simple but effective method for obtaining highly strain-relaxed InGaN buffers, called strain-relaxed templates (SRT), where the growth temperature of red LEDs can be as high as 870 °C with a 100% relaxed $In_{0.07}Ga_{0.93}N$ buffer [33]. In addition, LEDs with 0.31% EQE at 637 nm and a low forward voltage are reported based on SRT technology [34].

Although decent results of LEDs have been demonstrated based on this technology, laser diodes on an SRT have not been reported yet. In this work, we successfully demonstrate c-plane blue InGaN-based LDs grown on an SRT. A relaxation degree of 26.6% for the InGaN buffer was obtained, and by adopting a higher temperature and a thicker GaN growth in the SRT to reduce the defects, a smooth surface morphology of 0.65 nm root mean square (RMS) roughness was achieved. The lasing wavelength is 459 nm, and the threshold current density is 52 $kA/cm^2$ under the room temperature pulsed operation. The internal loss of the LDs on SRT was found to be 30–35 $cm^{-1}$, which is more than three times the value of the reference LDs without SRT. Regardless of the high threshold current density, these are the first demonstrated LDs using the strain-relaxed method on c-plane GaN.

## 2. Materials and Methods

The epi structure was grown by metal−organic chemical vapor deposition (MOCVD) on a c-plane freestanding bulk GaN substrate commercially available instead of sapphire, since the former provides less threading dislocation density in the substrate. Trimethylgallium (TMGa), triethylgallium (TEGa), trimethylindium (TMIn), ammonia ($NH_3$), disilane ($Si_2H_6$) and bis(cyclopentadienyl)magnesium (Cp2Mg) were used as the precursors and dopants. A 2.6 µm n-GaN layer was first grown at 1150 °C, and then a 3 nm InGaN decomposition layer (DL) was grown at 770 °C, followed by a low temperature GaN cap. After that, the temperature was ramped up to 1100 °C for a 700 nm thick n-GaN growth acting as a decomposition stop layer (DSL). During the growth of the DSL, the DL will be decomposed and form voids [35,36], providing the relaxation for the InGaN buffer which will be grown thereafter. We call the structure composed of decomposed DL, a GaN cap and DSL a strain-relaxed template (SRT). A 200 nm n-InGaN buffer of 20 periods of 5 nm InGaN and 5 nm GaN was then grown on top of the SRT. Next, a 60 nm n-InGaN consisting of 3 periods of 16 nm InGaN and 4 nm GaN was grown as the waveguide layer, followed by 4-period MQWs as the active region with a 2.5 nm low-temperature (LT) InGaN quantum well, 2 nm LT AlGaN and a 9 nm high-temperature (HT) GaN barrier in each period. After the MQWs growth, a 10 nm p-AlGaN electron blocking layer (EBL) was grown, followed by a 60 nm p-waveguide layer with the same structure and doping as the n-waveguide. Then, 210 nm p-GaN was grown as the p-cladding, and, finally, 15 nm p + GaN was grown as the p-contact layer. For comparison, a reference LD structure was also grown. Instead of growing a DL, a low-temperature (LT) GaN was grown while all the other layers were kept the same for fair comparison. The schematics of both LD structures are shown in Figure 1.

A high-resolution X-ray diffraction (HRXRD) reciprocal space map (RSM) was performed to analyze the relaxation of the InGaN buffer for both designs using the $(\bar{1}\bar{1}24)$ off-axis peak. Atomic force microscopy (AFM) was carried out to characterize the surface morphology of the samples. An on-wafer quick test was performed by putting indium dots

on the sample, and the electroluminescence (EL) spectrum was collected by an optical fiber and Ocean-Optics spectrometer.

Ridge stripe laser structures were fabricated in this work. The device process started with ridge etching by reactive ion etching (RIE) and a self-aligned liftoff process of the oxide insulator, followed by the deposition and etch of Indium Tin Oxide (ITO) as the p-contact and cladding layer. Due to its lower refractive index and resistance compared to GaN and its lower absorption loss compared to metal, ITO can provide a better confinement factor without significantly increasing the absorption loss and operating voltage [37]. A Ti/Au metal stack was then deposited as the metal pad for probing. Finally, both facets were formed by chemically assisted ion beam etching (CAIBE) with an Ar ion beam in a $Cl_2$ atmosphere [38], and backside Ti/Al/Ni/Au metal was deposited as the n-electrode.

The fabricated LDs were tested under pulse mode using a pulse generator with a pulse width of 500 ns and a duty cycle of 0.5%. The electroluminescence (EL) spectrum of LDs was collected by the same equipment mentioned above. The applied voltage and current were measured by the oscilloscope, and the light output power of the LDs was measured by an integrating sphere. The segmented contact method performed to measure the optical loss utilized the amplified spontaneous emission (ASE) spectra; the method and principles can be found in [39,40].

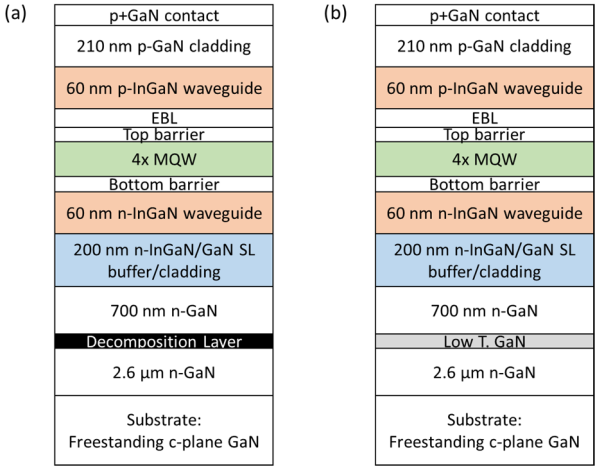


**Figure 1.** Schematic epi structure of (**a**) laser diodes on a strain-relaxed template (SRT) and (**b**) reference laser diodes. Instead of a decomposition layer, a low-temperature GaN was grown in reference LDs, while all other layers were kept the same.

## 3. Results and Discussion

The RSM of the $(\bar{1}\bar{1}24)$ off-axis peaks are shown in Figure 2a,b, which correspond to SRT LDs and reference LDs, respectively. From the results, we can extract the Indium content and the degree of relaxation in the InGaN layers on the SRT, where the buffer is 26.6% relaxed and contains 1.5% Indium, while the waveguide is 16.1% relaxed and has 4.3% Indium. In contrast to SRT LDs, the reference LDs show no relaxation, as shown in Figure 2b. The EL spectrum of the on-wafer quick test was also measured for both samples at a current density of 20 A/cm$^2$, as demonstrated in Figure 2c, where SRT LDs and reference LDs show an emission at 502.4 nm and 485.5 nm, respectively. The LD structure grown on SRT exhibits a red shift of 16.9 nm because of the relaxation of the InGaN layers underneath, enabling more Indium incorporation into the active region. It is important to note that, compared with our previous structure, the GaN DSL was grown much thicker and at a much higher temperature. There are two reasons behind this change. First, we found that, although a lower growth temperature of the DL and DSL can allow for a higher degree of relaxation, it is also accompanied by a higher defect density and a poor surface morphology, which are detrimental to lasers [36]. Hence, before optimizing the structure design to minimize defects and the poor morphology, we chose to grow at a

higher temperature for both the DL and DSL to reduce these issues but with a lower degree of relaxation. As shown in the atomic force microscopy (AFM) scan of the epi surface in Figure 2d, no v-pits are observed, and the surface morphology is smooth, with a root mean square (RMS) roughness of 0.65 nm. The second reason is because we found that the decomposed DL is highly absorbent due to phase separation and the formation of metallic Indium, which can be further confirmed by the sample picture in [36]. It is hence critical to grow a thick DSL to prevent the mode leaking into the DL and thus reduce the optical loss.

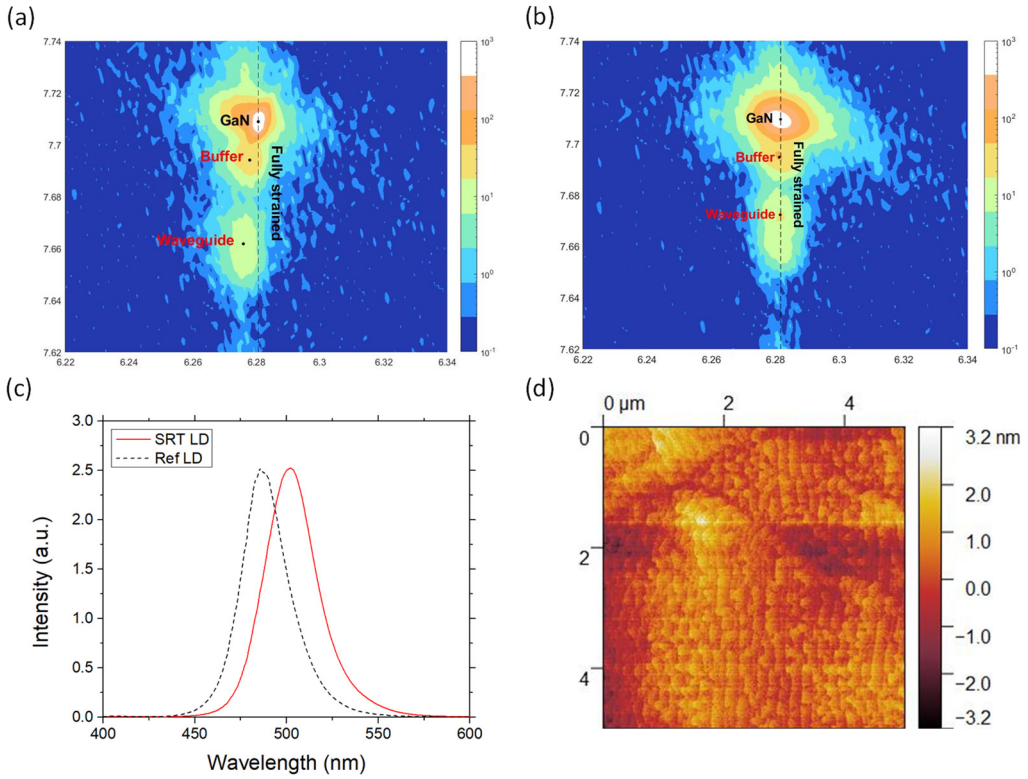


**Figure 2.** RSM of (**a**) SRT LDs: a 26.6% relaxed $In_xGa_{1-x}N$ buffer and a 16.1% relaxed $In_yGa_{1-y}N$ waveguide, with x = 0.015 and y = 0.043, respectively; and (**b**) reference LDs: the InGaN buffer and waveguide are both strained to GaN. (**c**) EL spectra at 20 A/cm$^2$ for SRT LDs and reference LDs, where the former show a 16.9 nm red shift. (**d**) A 5 by 5 μm$^2$ AFM scan on the top surface of the epi structure, showing a smooth morphology with an RMS roughness of 0.65 nm.

The schematic device structure of the processed SRT LD is shown in Figure 3a. Figure 3b presents the EL spectra before and after lasing. As the injected current reached the threshold condition, a sharp and narrow lasing peak at 459 nm was observed, and the far field pattern could be clearly seen, as shown in the inset of the figure. Figure 3c demonstrates the single facet light–current–voltage (L–I–V) characteristics of an 1800 μm cavity length and 1.5 μm ridge stripe width device. The threshold current is quite high at around 1405 mA, which corresponds to a current density of 52 kA/cm$^2$. Under the same testing setup, the reference LDs with the same laser ridge stripe configuration were also tested and already have a high threshold current density of 20 kA/cm$^2$ compared to other c-plane blue LD results, which implies that the non-optimized LD structure is one of the reasons for the high threshold of the LDs grown on the SRT. The lasing wavelength of the reference LDs is 456 nm, which is only 3 nm shorter than that of the SRT LDs. Note that the redshift of the SRT LDs is much smaller compared to the on-wafer quick test. The reason for this is the much higher threshold of the SRT results in more band filling effects and field screening, hence causing more of a blueshift of the lasing wavelength.

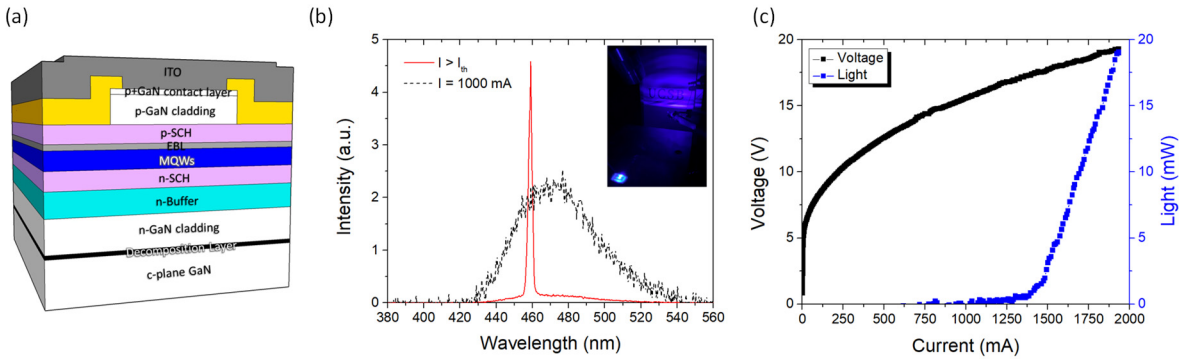


**Figure 3.** (**a**) Schematic of the device cross-section. (**b**) EL spectrum of the SRT LDs, showing a sudden drop in linewidth above the laser threshold. Inset: the observed far field pattern above the threshold. (**c**) Pulsed light-current-voltage (L-I-V) characteristics of a single facet of the 1800 × 1.5 $\mu m^2$ laser bar.

The segmented contact method was carried out to measure the gain and loss for both the SRT LDs and reference LDs. To have a fair comparison, the same ridge width (8 µm) was measured for both structures. The amplified spontaneous emission (ASE) spectra for $\Gamma g - \langle \alpha_i \rangle$ and $-\Gamma\alpha - \langle \alpha_i \rangle$ under various injection current densities of SRT LDs and reference LDs are shown in Figure 4a,b, respectively, where Γ is the confinement factor, g stands for gain, α stands for absorption and $\langle \alpha_i \rangle$ is the internal loss. As can be observed, the gain and loss curves merge well in the region below the band edge, where the internal loss $\langle \alpha_i \rangle$ of the material can be extracted. From the figure, it can be seen that the $\langle \alpha_i \rangle$ of the SRT lasers is 30–35 $cm^{-1}$, while for the reference lasers, it is about 10 $cm^{-1}$, which is less than one-third of the value. The much higher loss in the SRT LDs is the main reason why the threshold is much higher than that of the reference LDs. There are two possible reasons for the high internal loss in the SRT lasers: first, the threading dislocation density in the SRT template is still much higher than the reference sample, where a high density of threading dislocation can cause a significant amount of scattering loss [41]. Second, the tail of the optical mode might leak into the DL, which is highly optically absorbent. To confirm the loss from DL, a transmission measurement needs to be conducted to obtain the absorption coefficient of DL as well as the optical mode simulation. Future work on lowering $\langle \alpha_i \rangle$ is required to reduce the threshold current density and hence improve the device performance.

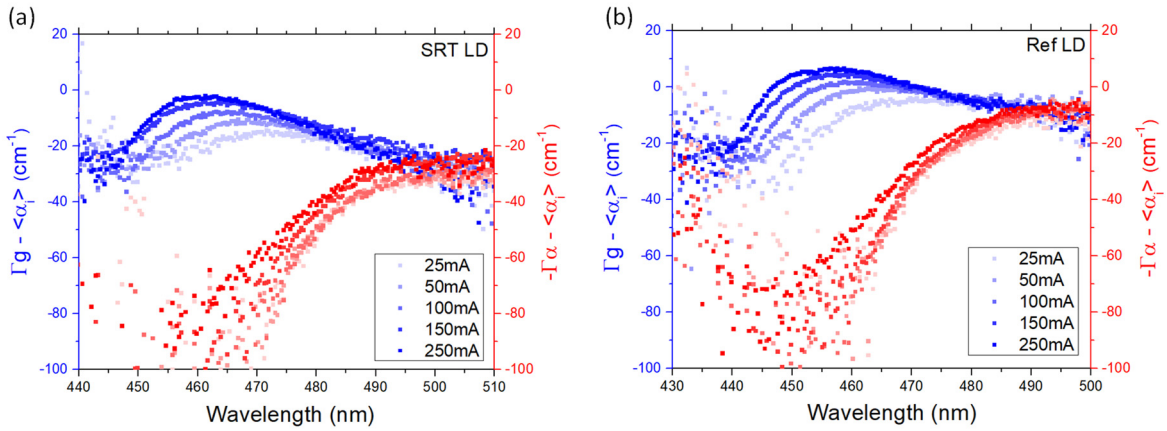


**Figure 4.** Results of the segmented contact measurement of (**a**) SRT LDs, (**b**) reference LDs. A three−times−higher internal loss is observed in the SRT lasers.

## 4. Conclusions

In summary, a c-plane blue laser diode grown on an SRT is demonstrated. The relaxation in the InGaN buffer is controlled within a small range before we can minimize the defects in it. The thickness of GaN DSL is designed to minimize the optical mode leaking

into the highly light-absorbent DL. The device demonstrates a threshold current density of 52 kA/cm$^2$ at a wavelength of 459 nm. From the segmented contact measurement, a more-than-three-times-higher loss in the SRT LDs compared to the reference LDs is identified, which is believed to be the main reason for the high threshold current density. Future work on optimizing the laser structure and minimizing internal loss is necessary to achieve a decent lasing threshold and extend the lasing wavelength.

**Author Contributions:** Formal analysis, H.-M.C.; investigation, H.-M.C.; data curation, H.-M.C., P.C.; software, P.C., N.L.; writing—original draft preparation, H.-M.C.; writing—review and editing, P.C., N.L., V.R.; visualization, H.-M.C.; supervision, S.N., S.P.D. and M.J.G.; project administration, S.N., S.P.D. and M.J.G.; funding acquisition, S.N., S.P.D. and M.J.G. All authors have read and agreed to the published version of the manuscript.

**Funding:** This work was supported by Google under Grant No. PO4100162358 and by the Defense Advanced Research Projects Agency (HR001120C0135). The results presented made use of the MRL Shared Experimental Facilities of UCSB, supported by the MRSEC program (NSF DMR 1720256), a member of the Materials Research Facilities Network (www.mrfn.org, accessed on April 2021), as well as the UCSB Nanofabrication Facility, an open access laboratory.

**Institutional Review Board Statement:** Not applicable.

**Informed Consent Statement:** Not applicable.

**Data Availability Statement:** The results presented in this paper are not available publicly at this time but may be obtained from the authors upon reasonable request.

**Conflicts of Interest:** The authors declare no conflict of interest.

## References

1. Hardy, M.T.; Feezell, D.F.; Denbaars, S.; Nakamura, S. Group III-nitride lasers: A materials perspective. *Mater. Today* **2011**, *14*, 408–415. [CrossRef]
2. Nakamura, S.; Senoh, M.; Nagahama, S.I.; Iwasa, N.; Yamada, T.; Matsushita, T.; Kiyoku, H.K.; Sugimoto, Y.S. InGaN-based multi-quantum-well-structure laser diodes. *Jpn. J. Appl. Phys.* **1996**, *35*, L74. [CrossRef]
3. Lutgen, S.; Avramescu, A.; Lermer, T.; Schillgalies, M.; Queren, D.; Müller, J.; Dini, D.; Breidenassel, A.; Strauss, U. Progress of blue and green InGaN laser diodes. In *Novel In-Plane Semiconductor Lasers IX*; SPIE: Bellingham, WA, USA, 2010; Volume 7616, pp. 89–96.
4. Lutgen, S.; Avramescu, A.; Lermer, T.; Queren, D.; Müller, J.; Bruederl, G.; Strauss, U. True green InGaN laser diodes. *Phys. Status solidi (a)* **2010**, *207*, 1318–1322. [CrossRef]
5. Raring, J.W.; Schmidt, M.C.; Poblenz, C.; Chang, Y.-C.; Mondry, M.J.; Li, B.; Iveland, J.; Walters, B.; Krames, M.R.; Craig, R.; et al. High-Efficiency Blue and True-Green-Emitting Laser Diodes Based on Non-*c*-Plane Oriented GaN Substrates. *Appl. Phys. Express* **2010**, *3*, 112101. [CrossRef]
6. Raring, J.W.; Hall, E.M.; Schmidt, M.C.; Poblenz, C.; Li, B.; Pfister, N.; Kebort, D.; Chang, Y.C.; Feezell, D.F.; Craig, R.; et al. State-of-the-art continuous-wave InGaN laser diodes in the violet, blue, and green wavelength regimes. In *Laser Technology for Defense and Security VI*; SPIE: Bellingham, WA, USA, 2010; Volume 7686, pp. 131–140.
7. Kozaki, T.; Matsumura, H.; Sugimoto, Y.; Nagahama, S.-I.; Mukai, T. High-power and wide wavelength range GaN-based laser diodes. In *Novel In-Plane Semiconductor Lasers V*; SPIE: Bellingham, WA, USA, 2006; Volume 6133, pp. 16–27.
8. Kozaki, T.; Yanamoto, T.; Miyoshi, T.; Fujimura, Y.; Nagahama, S.I.; Mukai, T. *52.3: High-Power InGaN Blue-Laser Diodes for Displays. In SID Symposium Digest of Technical Papers*; Blackwell Publishing Ltd.: Oxford, UK, 2005; Volume 36, pp. 1605–1607.
9. Okamoto, K.; Kashiwagi, J.; Tanaka, T.; Kubota, M. Nonpolar m-plane InGaN multiple quantum well laser diodes with a lasing wavelength of 499.8 nm. *Appl. Phys. Lett.* **2009**, *94*, 071105. [CrossRef]
10. Okamoto, K.; Ohta, H.; Chichibu, S.F.; Ichihara, J.; Takasu, H. Continuous-wave operation of m-plane InGaN multiple quantum well laser diodes. *Jpn. J. Appl. Phys.* **2007**, *46*, L187. [CrossRef]
11. Adachi, M.; Yoshizumi, Y.; Enya, Y.; Kyono, T.; Sumitomo, T.; Tokuyama, S.; Takagi, S.; Sumiyoshi, K.; Saga, N.; Ikegami, T.; et al. Low threshold current density InGaN based 520–530 nm green laser diodes on semi-polar {2021} free-standing GaN substrates. *Appl. Phys. Express* **2010**, *3*, 121001. [CrossRef]
12. Takagi, S.; Enya, Y.; Kyono, T.; Adachi, M.; Yoshizumi, Y.; Sumitomo, T.; Yamanaka, Y.; Kumano, T.; Tokuyama, S.; Sumiyoshi, K.; et al. High-power (over 100 mW) green laser diodes on semipolar {2021} GaN substrates operating at wavelengths beyond 530 nm. *Appl. Phys. Express* **2012**, *5*, 082102. [CrossRef]
13. Feezell, D.F.; Schmidt, M.C.; Farrell, R.M.; Kim, K.C.; Saito, M.; Fujito, K.; Cohen, D.A.; Speck, J.S.; DenBaars, S.P.; Nakamura, S. AlGaN-cladding-free nonpolar InGaN/GaN laser diodes. *Jpn. J. Appl. Phys.* **2007**, *46*, L284. [CrossRef]

14. Lin, Y.D.; Hardy, M.T.; Hsu, P.S.; Kelchner, K.M.; Huang, C.Y.; Haeger, D.A.; Farrell, R.M.; Fujito, K.; Chakraborty, A.; Ohta, H.; et al. Blue-green InGaN/GaN laser diodes on miscut m-plane GaN substrate. *Appl. Phys. Express* **2009**, *2*, 082102. [CrossRef]
15. Tyagi, A.; Farrell, R.M.; Kelchner, K.M.; Huang, C.Y.; Hsu, P.S.; Haeger, D.A.; Hardy, M.T.; Holder, C.; Fujito, K.; Cohen, D.A.; et al. AlGaN-cladding free green semipolar GaN based laser diode with a lasing wavelength of 506.4 nm. *Appl. Phys. Express* **2009**, *3*, 011002. [CrossRef]
16. Hardy, M.T.; Wu, F.; Shan Hsu, P.; Haeger, D.A.; Nakamura, S.; Speck, J.S.; DenBaars, S.P. True green semipolar InGaN-based laser diodes beyond critical thickness limits using limited area epitaxy. *J. Appl. Phys.* **2013**, *114*, 183101. [CrossRef]
17. Sun, Y.; Zhou, K.; Feng, M.; Li, Z.; Zhou, Y.; Sun, Q.; Liu, J.; Zhang, L.; Li, D.; Sun, X.; et al. Room-temperature continuous-wave electrically pumped InGaN/GaN quantum well blue laser diode directly grown on Si. *Light Sci. Appl.* **2018**, *7*, 13. [CrossRef] [PubMed]
18. Jiang, L.; Liu, J.; Tian, A.; Cheng, Y.; Li, Z.; Zhang, L.; Zhang, S.; Li, D.; Ikeda, M.; Yang, H. GaN-based green laser diodes. *J. Semicond.* **2016**, *37*, 111001. [CrossRef]
19. Ho, I.; Stringfellow, G.B. Solid phase immiscibility in GaInN. *Appl. Phys. Lett.* **1996**, *69*, 2701–2703. [CrossRef]
20. Matsuoka, T.; Yoshimoto, N.; Sasaki, T.; Katsui, A. Wide-gap semiconductor InGaN and InGaAlN grown by MOVPE. *J. Electron. Mater.* **1992**, *21*, 157–163. [CrossRef]
21. Pereira, S.; Correia, M.R.; Pereira, E.; O'donnell, K.P.; Trager-Cowan, C.; Sweeney, F.; Alves, E. Compositional pulling effects in Inx Ga1− xN/GaN layers: A combined depth-resolved cathodoluminescence and Rutherford backscattering/channeling study. *Phys. Rev. B* **2001**, *64*, 205311. [CrossRef]
22. Hiramatsu, K.; Kawaguchi, Y.; Shimizu, M.; Sawaki, N.; Zheleva, T.; Davis, R.F.; Tsuda, H.; Taki, W.; Kuwano, N.; Oki, K. The composition pulling effect in MOVPE grown InGaN on GaN and AlGaN and its TEM characterization. *MRS Internet J. Nitride Semicond. Res.* **1997**, *2*, 11. [CrossRef]
23. Der Maur, M.A.; Pecchia, A.; Penazzi, G.; Rodrigues, W.; Di Carlo, A. Efficiency drop in green InGaN/GaN light emitting diodes: The role of random alloy fluctuations. *Phys. Rev. Lett.* **2016**, *116*, 027401. [CrossRef]
24. Waltereit, P.; Brandt, O.; Trampert, A.; Grahn, H.T.; Menniger, J.; Ramsteiner, M.; Reiche, M.; Ploog, K.H. Nitride semiconductors free of electrostatic fields for efficient white light-emitting diodes. *Nat.* **2000**, *406*, 865–868. [CrossRef]
25. Scheibenzuber, W.G.; Schwarz, U.T.; Veprek, R.G.; Witzigmann, B.; Hangleiter, A. Calculation of optical eigenmodes and gain in semipolar and nonpolar InGaN/GaN laser diodes. *Phys. Rev. B* **2009**, *80*, 115320. [CrossRef]
26. Lermer, T.; Schillgalies, M.; Breidenassel, A.; Queren, D.; Eichler, C.; Avramescu, A.; Müller, J.; Scheibenzuber, W.; Schwarz, U.; Lutgen, S.; et al. Waveguide design of green InGaN laser diodes. *Phys. Status solidi (a)* **2010**, *207*, 1328–1331. [CrossRef]
27. Hestroffer, K.; Wu, F.; Li, H.; Lund, C.; Keller, S.; Speck, J.S.; Mishra, U.K. Relaxed c-plane InGaN layers for the growth of strain-reduced InGaN quantum wells. *Semicond. Sci. Technol.* **2015**, *30*, 105015. [CrossRef]
28. Even, A.; Laval, G.; LeDoux, O.; Ferret, P.; Sotta, D.; Guiot, E.; Levy, F.; Robin, I.C.; Dussaigne, A. Enhanced In incorporation in full InGaN heterostructure grown on relaxed InGaN pseudo-substrate. *Appl. Phys. Lett.* **2017**, *110*, 262103. [CrossRef]
29. Keller, S.; Lund, C.; Whyland, T.; Hu, Y.; Neufeld, C.; Chan, S.; Wienecke, S.; Wu, F.; Nakamura, S.; Speck, J.S.; et al. InGaN lattice constant engineering via growth on (In, Ga) N/GaN nanostripe arrays. *Semicond. Sci. Technol.* **2015**, *30*, 105020. [CrossRef]
30. Pasayat, S.S.; Gupta, C.; Wang, Y.; DenBaars, S.P.; Nakamura, S.; Keller, S.; Mishra, U.K. Compliant micron-sized patterned InGaN pseudo-substrates utilizing porous GaN. *Materials* **2020**, *13*, 213. [CrossRef]
31. Pasayat, S.S.; Ley, R.; Gupta, C.; Wong, M.S.; Lynsky, C.; Wang, Y.; Gordon, M.J.; Nakamura, S.; Denbaars, S.P.; Keller, S.; et al. Color-tunable < 10 μ m square InGaN micro-LEDs on compliant GaN-on-porous-GaN pseudo-substrates. *Appl. Phys. Lett.* **2020**, *117*, 061105.
32. White, R.C.; Li, H.; Khoury, M.; Lynsky, C.; Iza, M.; Keller, S.; Sotta, D.; Nakamura, S.; DenBaars, S.P. InGaN-Based microLED Devices Approaching 1% EQE with Red 609 nm Electroluminescence on Semi-Relaxed Substrates. *Crystals* **2021**, *11*, 1364. [CrossRef]
33. Chan, P.; Rienzi, V.; Lim, N.; Chang, H.M.; Gordon, M.; DenBaars, S.P.; Nakamura, S. Demonstration of relaxed InGaN-based red LEDs grown with high active region temperature. *Appl. Phys. Express* **2021**, *14*, 101002. [CrossRef]
34. Wong, M.S.; Chan, P.; Lim, N.; Zhang, H.; White, R.C.; Speck, J.S.; Denbaars, S.P.; Nakamura, S. Low Forward Voltage III-Nitride Red Micro-Light-Emitting Diodes on a Strain Relaxed Template with an InGaN Decomposition Layer. *Crystals* **2022**, *12*, 721. [CrossRef]
35. Smalc-Koziorowska, J.; Grzanka, E.; Lachowski, A.; Hrytsak, R.; Grabowski, M.; Grzanka, S.; Kret, S.; Czernecki, R.; Turski, H.; Marona, L.; et al. Role of Metal Vacancies in the Mechanism of Thermal Degradation of InGaN Quantum Wells. *ACS Appl. Mater. Interfaces* **2021**, *13*, 7476–7484. [CrossRef] [PubMed]
36. Chan, P.; DenBaars, S.P.; Nakamura, S. Growth of highly relaxed InGaN pseudo-substrates over full 2-in. wafers. *Appl. Phys. Lett.* **2021**, *119*, 131106. [CrossRef]
37. Mehari, S.; Cohen, D.A.; Becerra, D.L.; Nakamura, S.; DenBaars, S.P. Demonstration of enhanced continuous-wave operation of blue laser diodes on a semipolar 202¯ 1¯ GaN substrate using indium-tin-oxide/thin-p-GaN cladding layers. *Opt. Express* **2018**, *26*, 1564–1572. [CrossRef] [PubMed]
38. Kuritzky, L.Y.; Becerra, D.L.; Abbas, A.S.; Nedy, J.; Nakamura, S.; Denbaars, S.; A Cohen, D. Chemically assisted ion beam etching of laser diode facets on nonpolar and semipolar orientations of GaN. *Semicond. Sci. Technol.* **2016**, *31*, 075008. [CrossRef]

39. Blood, P.; Lewis, G.; Smowton, P.M.; Summers, H.; Thomson, J.; Lutti, J. Characterization of semiconductor laser gain media by the segmented contact method. *IEEE J. Sel. Top. Quantum Electron.* **2003**, *9*, 1275–1282. [CrossRef]
40. Li, H.; Li, P.; Zhang, H.; Nakamura, S.; DenBaars, S.P. Demonstration of Efficient Semipolar 410 nm Violet Laser Diodes Heteroepitaxially Grown on High-Quality Low-Cost GaN/Sapphire Substrates. *ACS Appl. Electron. Mater.* **2020**, *2*, 1874–1879. [CrossRef]
41. Liau, Z.L.; Aggarwal, R.L.; Maki, P.A.; Molnar, R.J.; Walpole, J.N.; Williamson, R.C.; Melngailis, I. Light scattering in high-dislocation-density GaN. *Appl. Phys. Lett.* **1996**, *69*, 1665–1667. [CrossRef]